Pneumatically actuated elastomeric device for simultaneous mechanobiological studies & live-cell fluorescent microscopy

Pneumatically actuated elastomeric device for simultaneous mechanobiological studies and live-cell fluorescent microscopy

Joose Kreutzer, Marlitt Viehrig, Antti-Juhana Mäki, Pasi Kallio
Biomedical Sciences and Technology, BioMediTech
Tampere University of Technology
Tampere, Finland
joose.kreutzer@tut.fi, pasi.kallio@tut.fi

Rolle Rahikainen, Vesa Hytönen
Protein Dynamics group, BioMediTech
University of Tampere
Tampere, Finland
vesa.hytonen@uta.fi

***Abstract*— In this study, we demonstrate the functionality and usability of a compact, pneumatically actuated, elastomeric stimulation device for mechanobiological studies. The soft mechatronic device enables high-resolution live-cell confocal fluorescent imaging during equiaxial stretching. Several single cells can be tracked and imaged repeatedly after stretching periods. For demonstration, we provide image based analysis of dynamic change of the cell body and the nucleus area and actin fiber orientation during mechanical stimulation of mouse embryonic fibroblast (MEF) cells. Additionally, we present the characteristics of the device utilizing computational simulations and experimental validation using a particle tracking method for strain field analysis.**

Keywords*— high-resolution imaging; mechanical stimulation; mouse embryonic fibroblasts, particle tracking; PDMS; pneumatic actuation; strain field analysis

I. Introduction

Mechanical stimulation of cells affects, for example, cell morphology, orientation, focal adhesion, and fate of differentiated stem cells, as has been shown in recent publications [1-3]. Several approaches of applying mechanical stimuli to cells have been reported, such as flow-induced shear forces, hydrostatic pressure, substrate topography, stiffness, cell indentation, and substrate stretching [4]. Mechanobiological studies are important for understanding the molecular mechanisms of cells sensing and responding to mechanical signals. To visualize the response of cells to mechanical stimulation a high-resolution imaging and real-time observation are essential. In this paper, we concentrate on a substrate stretching method and introduce a pneumatically operated soft mechatronic device capable for real-time multi-cell high-resolution confocal fluorescent imaging during stretching.

A few research groups have reported on custom-made stretching systems. A typical approach is to apply electro-mechanical actuators to stretch the substrate, such as DC- or stepper-motors [5, 6]. It might be difficult to provide stretching for multiple cultures at the same time and/or integrate such a setup easily to a microscope environment. Furthermore, such a setup can not be used in a humid environment due to a high risk for corrosion in electrical and mechanical parts and thus, a high contamination risk.

Few research groups have demonstrated the cell stretching methods utilizing pneumatic actuation and biocompatible materials [7-10]. Pneumatic actuation is easy to apply in an incubator environment or in a microscope environment. Also, pneumatic actuation can be easily utilized in high-throughput applications [7]. However, common for all the current devices is that high-resolution imaging is disturbed because of multiple interfaces and materials between the cells and the microscope objective. Furthermore, in some approaches cells must be plated inside a tiny channel where additional continuous perfusion or frequent medium change is required to maintain the cells for a longer period of time [8,9]. In other approaches, lubricant oil is required to operate the stretching device [7,10]. Also, commercially available cell substrate stretching devices are lacking capabilities to trace cells with high-resolution imaging. For example, the commercial Flexcell® device requires a loading post below the stretching substrate, which completely blocks visualization of the cells using inverted microscopy. Thus, an important bottleneck in the current cell stretching systems is their incapability for characterizing in situ the influences of stretching at a single cell level.

In this paper, we introduce an innovative and easy to use soft mechatronic cell stretching device that enables high resolution imaging during stretching. We demonstrate its usability for high-resolution differential interference contrast (DIC) and fluorescent imaging of multiple cells during mechanical stretching and provide examples of further analysis possibilities.

II. Methods

A. Design and Fabrication of Stretching Device

Stretching devices (see Fig. 1A) were fabricated using polydimethylsiloxane (PDMS, Sylgard 184, Dow Corning, USA) and glass similarly as shown previously in [11,12]. Briefly, the stretching device has a circular cultivation area of

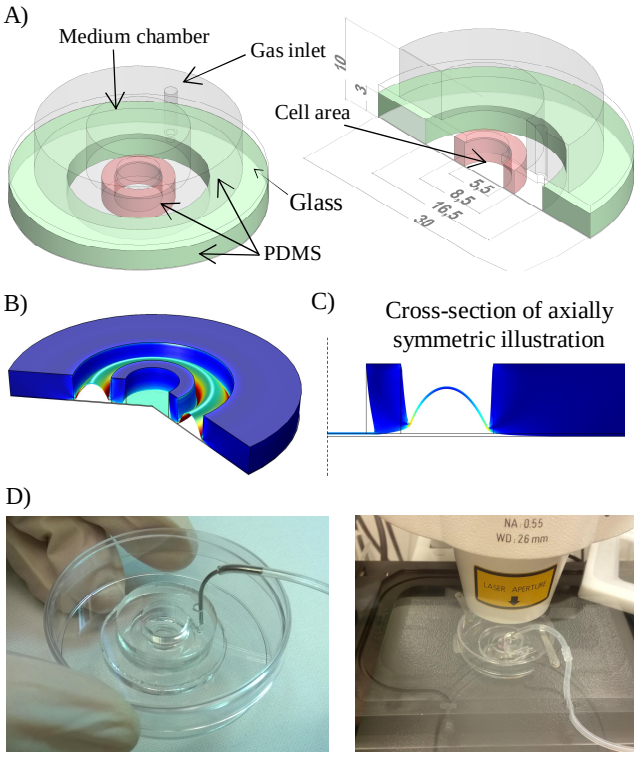

Fig. 1. A) Schematic picture of the stretching device and dimensions in [mm]. B) Simulated illustration of a simplified stretching device used for computational simulations. C) 2D cross-section of axially symmetric simulated illustration. D) Real setup on Petri dish and on microscope. Connected stretching device in secured Petri dish holder. The tubing is secured to the heating insert of the microscope stage. A lid for CO_2 supply can be added on top.

A = 23.8 mm^2 (d = 5.5 mm, h = 3 mm) implemented on a PDMS membrane (cell stretching substrate) with a thickness of t = 0.12 mm. The PDMS pieces were punched out from a bulk PDMS sheet utilizing custom made punches with diameters of 5.5 mm, 8.5 mm, 16 mm, and 30 mm. Glass plates were ordered from Aki-lasi Oy (Tampere, Finland) and holes were drilled for the gas inlet and the cell plating area. All pieces were bonded permanently together using oxygen plasma (Pico-SR-PCCE, Diener Electronic, Ebhausen, Germany) with the following parameters: power 30 W, chamber pressure 0.30 mbar, O_2 gas flow rate 1.4 sccm, and time 20 s for PDMS – PDMS bonds and 15 s for PDMS – glass bonds.

Stretching devices were operated by applying partial pressure between two concentric rings. Partial vacuum deflects the membrane and the inner ring expands (See Fig. 1B and 1C). Partial vacuum pressure was generated utilizing a custom made electro-pneumatic transducer platform as previously reported in [11].

B. Characterization of Stretching Device

Computational simulation and experimental validation were used to characterize the stretching device. COMSOL Multiphysics® 5.1 (COMSOL Inc., USA) was used for numerical simulations to estimate the strain field of the cell stretching substrate. Solid Mechanics physics with hyperelastic (Neo-Hookean model) and incompressible material property of PDMS was used for modelling. Other material parameters used were following: Young's modulus (2 MPa), Lamé parameter (667e3 N/m^2), bulk modulus (333.3 MPa), and density (971 kg/m^3).

Two fabricated stretching devices were experimentally characterized to validate the computational simulation. Green fluorescent polystyrene particles (d = 4.18 ± 0.397 µm, c = 7 µl/ml in DI-water, Dragon Green, Bangs Laboratories Inc.) were unspecific absorbed to the PDMS substrate. The substrate was then stretched with nine static partial vacuum pressure settings ranging from 0 to 400 mbar in 50 mbar increments. The substrate was then imaged with each applied partial vacuum pressure using an inverted optical microscope (Zeiss Axio Observer.Z1, Carl Zeiss Microscopy, Jena, Germany). 10x magnification and stitching were used for generating the images. The in-plane strain field of the stretched substrate was analyzed using particle tracking algorithms of Fiji (open source image processing software).

C. Functionalization of Stretching Substrate

The stretching substrates were functionalized with fibronectin by physisorption. PDMS substrates were covered with 50 µg/ml of affinity purified human fibronectin in PBS (pH 7.4), followed by 15 min incubation in a 37 ℃ incubator and another 15 min in a laminar hood at room temperature. During the second incubation, the stretching devices were sterilized by exposing them to UV-light. After the incubation, the fibronectin solution was removed and the stretching devices were washed once with PBS.

D. Cell Line and Expression Constructs

Wild type mouse embryonic fibroblast (MEF) cells were used to demonstrate the feasibility of combining live cell imaging and simultaneous cell stretching. The cells were co transfected with plasmids expressing LifeAct-GFP (Visualization of actin cytoskeleton) and Histone-H2B-mCherry (Visualization of the nucleus) by using Neon Transfection System (Thermo Fisher Scientific). The transfected cells were allowed to recover for 48 hours before plating them on stretching devices. 15 000 cells were plated within 55 µl medium. Cells were allowed to attach for three hours before stretching experiment was started.

E. Live Cell Imaging Setup

An inverted Zeiss Cell Observer.Z1 (Carl Zeiss Microscopy, Jena, Germany) microscope equipped with LMS780 confocal unit, incubator cage (37 ℃, 5% CO_2), and Zeiss Plan-Apochromat 63x/ NA1.2 W objective was used for live cell imaging. Immersol G was used as immersion liquid (Zeiss 462959-9901-000). LifeAct-GFP and H2B-mCherry were excited with 488 nm argon laser and 594 nm helium-neon laser, respectively.

Prior to imaging, stretching devices were placed in a 50 mm Petri dish with a hole in the bottom to allow for a direct contact between the immersion liquid and the stretching substrate. A vacuum connection pipe was applied through the lid of the Petri dish (See Fig. 1D). Thus, the culture was sealed against contaminations. The Petri dish was then placed on the microscope.

In this demonstration, seven cells around the well (5.5 mm in diameter) were tracked. The position coordinates of those cells were stored at the beginning of experiment and the same positions were located semiautomatically after every stretching period. For each position, a Z-stack of 16 images with 0.5 µm intervals was created. Imaged field size was 67.3 µm x 67.3 µm and the used pixel size 130.2 nm.

F. Stretching Parameters

In this demonstration, we used 0.5 Hz sinusoidal waveform with 5 % strain amplitude. During the image acquisition, a static pre-stretch of 1.5 % was used to minimize substrate movements. We used four different imaging time points: 0 min, 10 min, 30 min and 60 min. At the beginning of stretching, lower strain amplitudes were used to adapt the cells to the strain (1.5 % for 1 min and 3 % for 2 min at 0.5 Hz). Subsequently, cells were stretched with 0.5 Hz and 5 % amplitude for 7 min until the second imaging time point (10 min). Rest of the experiment was performed with 5 % strain amplitude and 0.5 Hz.

G. Cell Analysis

The open source image processing software Fiji [13] was utilized in the analysis of cell morphology. Software was applied to determine the size of a cell and its nucleus using a selected region of interest (ROI) and actin fiber orientation data. To minimize errors caused by possible sample movement on the Z-axis, maximal intensity projection was performed to all raw data utilizing incorporated image processing functions in Fiji.

To determine the surface area of each cell, intensity thresholding was used to remove the image background. The outer border of the cell was defined as a ROI by applying the ROI manager integrated in Fiji.

Actin fiber orientation was characterized by using the open source Directionality plug-in for Fiji [14]. Hereby, a Fourier gradient is applied to the image to analyze the main direction of the actin fibers. The main fiber orientations are summarized in a histogram given out by the plug-in.

III. Results and Discussions

A. Characterization of Stretching Device

The computational simulation of the strain field shows that the strain is equal in the cell culture substrate. The maximum strain value in simulation was 12.1 % for this stretching device (See Fig. 2). Similar results were obtained utilizing particle tracking on the culture substrate. The two samples of the characterized stretching devices provided maximum strains of 10.4 % ± 0.08 % (Sample 1) and 11.5 % ± 0.21 % (Sample 2) (See Fig 2). Small variations in the strain field come mostly from the manufacturing of the stretching devices. In manual punching, dimensions of the devices slightly differ from the ideal structure. However, variations are still relatively small between the devices and computational results. Also, within one device, the deviation is very small (0.1 % – 0.2 %).

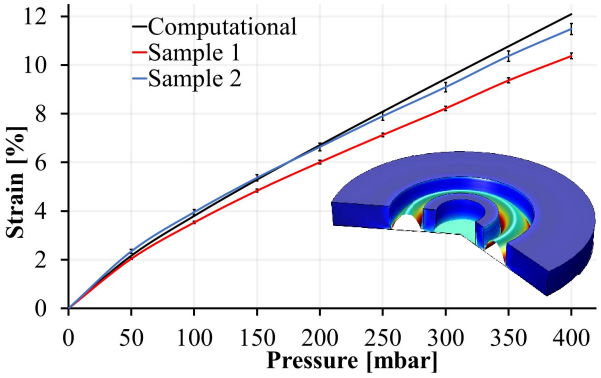

Fig. 2. Strain results. Computational strain analysis and validated strain field results from two different stretching device.

We also demonstrated that the cell substrate returns to its original position after stretching, which allows repeated imaging of single cells. By storing the position coordinates for the imaged cells at the beginning of the experiment, each position can be re-imaged later at desired intervals. This makes analysis much faster and more cells can be analyzed.

B. Cell Analysis

To demonstrate the excellent optical capabilities of our system, we demonstrate its compatibility with confocal fluorescence microscopy. Importantly, we demonstrate simultaneous imaging of multiple fluorescence channels and a DIC image during device stretching experiments (See Fig 3).

In analysis of cell samples, the definition of cells as ROIs is a key feature for more detailed characterization, including surface area measurements, cell counting, mask formation, and batch processing to just name a few. We successfully defined single cell ROIs by adjusting the image threshold to get the exact cellular borders (See Figure 3). The cell surface area analysis of five cells using ROI definition has been done using the measurement capabilities of Fiji. Two analysis out of seven was not successful because some cells were partially overlapping other cell or moved out of the imaging window. Results are shown in Fig. 4A.

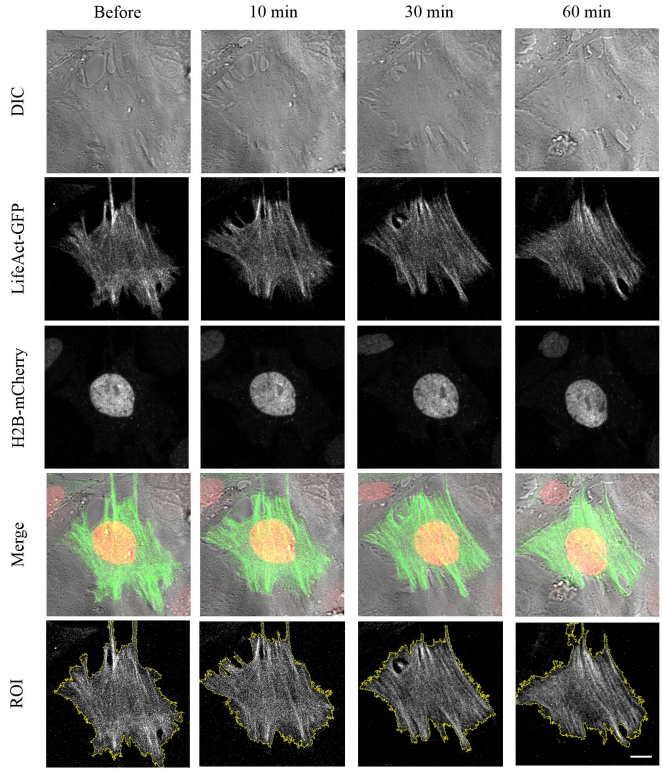

Fig. 3. Confocal fluorescence microscopy images before and after 10, 30, and 60 min of stretching. Demonstrated capability of the system to obtain multiple fluorescence channels and a DIC image simultaneously. ROI maps of cells shown in the bottom line. Scale bar in the bottom right corner 10 µm. All images are same size (67.3 µm x 67.3 µm).

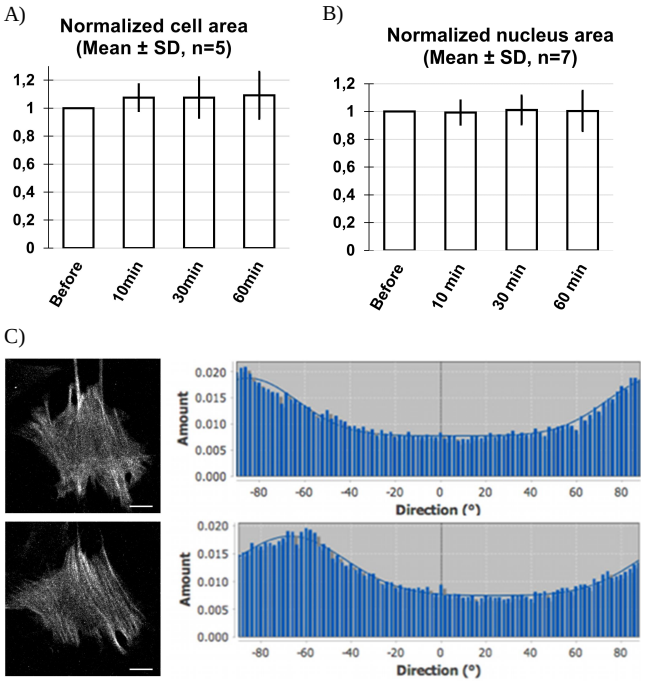

Fig. 4. Analysis of cell adhesion area, nucleus area, and fiber orientation. A) Average of projected area of cell adhesion is slightly increasing (statistically non-significant changes). B) Average of projected area of nucleaus remains the same but variation of area increase. C) Directionality analysis of actin fibre orientation inside cells before and after 60 min stretching. Actin filament orientation remains non-directional. Scalebar is 10 µm.

When stretching a flexible substrate equiaxially, it expands equally in all directions. Hence, the same increase in surface area should become visible in the stretched cells. Cells, as adaptable structures, re-organize with the applied strain and change their appearance. To secure their surface attachment during strain application to the cellular matrix, cytoskeletal microstructures adapt and flatten the cell. This might lead to a slight increase in the cell surface area during strain application. The cell surface area indeed slightly increases on average (9.2 % ± 16.8 %) during the stretching experiments as illustrated in Fig. 4A. However, variation in the results is relatively high and the increase in the cell area was not statistically significant.

As another example, we also studied how substrate stretching affects the projected size of cell nucleus. As a cell adapts to the repeated substrate stretching, cellular tension increases to match the substrate properties. This tension is also transmitted to the nuclear proteins and may therefore affect nucleus thickness and its projected size. However, we did not observe any changes in the nucleus size after 60 min of stretching (0.4 % ± 14.4 %) with the parameters mentioned above (See Fig 4B).

The actin skeleton of eukaryotic cells is responsible for various motility related cellular functions, such as cellular movement, cell division, intracellular transport and cell signaling. Actin fibers form majorly along the main strain axis, which also represents the main orientation axis of the cell, and at the outer edge of a cell for stability. Mechanical stimulation should cause the actin cytoskeleton to reorganize and react to the applied strain. During equiaxial stretching a diversity of strain axis should form next to the main strain axis inside the cell. To demonstrate the suitability of the cell stretching device for microscopically analyzing actin fiber orientation, we analyzed the actin fiber directionality using a standard Fiji plug-in (See Fig. 4C). Hereby, it becomes clear that the orientation of actin filaments remains non-directional and equiaxial after 60 min of stretching. The main orientation of the cell is visible as a wide peak.

IV. CONCLUSION

We demonstrated the usability of the pneumatically actuated stretching device for fluorescent confocal imaging of living MEF cells during mechanical stimulation. This is an important step in advancing single cell mechanobiological studies with high-resolution imaging during stretching. The presented technology provides outstanding tool to visualize the response of cells to mechanical stimulation with high-resolution imaging and real-time observation. In addition, the system allows to save the position coordinates of cells and track the cells immediately after stretching cycle. Therefore, it

is possible to image several cells semiautomatically and gain throughput of the study. Furthermore, different cell analysis protocols can be exploited due to the high quality images. This was demonstrated using two different fluorescent markers for live cell imaging and analyzing briefly the actin fibres and their orientation, size of cell body and nucleus. Additionally, the device fits to standard Petri dish frames that allows easy installation to most inverted microscopes and is also compatible with stage-top incubator systems used in live-cell imaging. Moreover, parallel devices can be used in long-term experiments inside the incubator with controlled stretching parameters. Entire stretching system also enables different stretching waveforms, frequencies, and strain amplitudes for further stimulation and analysis of cells.

ACKNOWLEDGMENT

The study was part of the "Human Spare Parts" project funded by the Finnish Funding Agency for Technology and Innovation (TEKES). The research was financially supported by Academy of Finland (grant 290506), The Finnish Cultural Foundation (The Pirkanmaa Regional Fund).

REFERENCES

[1] S.-J. Gwak, S. H. Bhang, I.-K. Kim, S.-S. Kim, S.-W. Cho, O. Jeon, K. J. Yoo, A. J. Putnam, and B.-S. Kim, "The effect of cyclic strain on embryonic stem cell-derived cardiomyocytes," *Biomaterials*, vol. 29, no. 7, pp. 844–56, Mar. 2008.

[2] T. M. Maul, D. W. Chew, A. Nieponice, and D. A. Vorp, "Mechanical stimuli differentially control stem cell behavior: morphology, proliferation, and differentiation," *Biomech. Model. Mechanobiol.*, vol. 10, no. 6, pp. 939–53, Dec. 2011.

[3] D. a. Lee, M. M. Knight, J. J. Campbell, and D. L. Bader, "Stem cell mechanobiology," *J. Cell. Biochem.*, vol. 112, no. 1, pp. 1–9, Jan. 2011

[4] D.-H. Kim, P. K. Wong, J. Park, A. Levchenko, and Y. Sun, "Microengineered platforms for cell mechanobiology," Annu. Rev. Biomed. Eng., vol. 11, pp. 203–33, Jan. 2009.

[5] W. W. Ahmed, M. H. Kural, and T. A. Saif, "A novel platform for in situ investigation of cells and tissues under mechanical strain," *Acta Biomater.*, vol. 6, no. 8, pp. 2979–90, Aug. 2010.

[6] L. Huang, P. S. Mathieu, and B. P. Helmke, "A stretching device for high-resolution live-cell imaging," *Ann. Biomed. Eng.*, vol. 38, no. 5, pp. 1728–40, May 2010

[7] C. Moraes, J.-H. Chen, Y. Sun, and C. A. Simmons, "Microfabricated arrays for high-throughput screening of cellular response to cyclic substrate deformation.," *Lab Chip*, vol. 10, no. 2, pp. 227–34, Jan. 2010

[8] D. Huh, B. D. Matthews, A. Mammoto, M. Montoya-Zavala, H. Y. Hsin, and D. E. Ingber, "Reconstituting organ-level lung functions on a chip," *Science*, vol. 328, no. 5986, pp. 1662–1668, 2010.

[9] D. Tremblay, S. Chagnon-Lessard, M. Mirzaei, A. E. Pelling, and M. Godin, "A microscale anisotropic biaxial cell stretching device for applications in mechanobiology," *Biotechnol. Lett.*, vol. 36, no. 3, pp. 657–665, Mar. 2014.

[10] D. Wang, Y. Xie, B. Yuan, J. Xu, P. Gong, and X. Jiang, "A stretching device for imaging real-time molecular dynamics of live cells adhering to elastic membranes on inverted microscopes during the entire process of the stretch.," *Integr. Biol.*, vol. 2, no. 5–6, pp. 288–93, Jun. 2010.

[11] J. Kreutzer, L. Ikonen, J. Hirvonen, M. Pekkanen-Mattila, K. Aalto-Setälä, and P. Kallio, "Pneumatic cell stretching system for cardiac differentiation and culture.," *Med. Eng. Phys.*, vol. 36, pp. 496–501, Oct. 2014.

[12] F. Zhao, J. Kreutzer, and P. Kallio, "Computational modeling and structural improvement of a pneumatically actuated concentric double-shell structure for cell stretching," in *2014 Proc. IEEE Int. Conf. Mechatronics and Automation (ICMA)*, pp. 906–911.

[13] J. Schindelin, I. Arganda-Carreras, E. Frise, V. Kaynig, M. Longair, T. Pietzsch, S. Preibisch, C. Rueden, S. Saalfeld, B. Schmid, J.-Y. Tinevez, D. J. White, V. Hartenstein, K. Eliceiri, P. Tomancak, A. Cardona, "Fiji: an open-source platform for biological-image analysis" *Nature Methods* 9, 2012, pp: 676–682.

[14] J.-Y. Tinevez. "Directionality (Fiji)", Fiji Plug-In, 2010